JOURNAL OF MATERIALS SCIENCE **36** (2001) 3253–3260

Hydroxy- and fluorapatite films on Ti alloy substrates: Sol-gel preparation and characterization

M. CAVALLI, G. GNAPPI, A. MONTENERO*
Dipartimento di Chimica Generale e Inorganica, Chimica Analitica e Chimica Fisica, Università di Parma, Parco Area delle Scienze 17/A, 43100 Parma, Italy
E-mail: monte@unipr.it

D. BERSANI, P. P. LOTTICI
Istituto Nazionale per la Fisica della Materia e Dipartimento di Fisica, Università di Parma, Parco Area delle Scienze 7A, 43100 Parma, Italy

S. KACIULIS, G. MATTOGNO
ICMAT-CNR, Via Salaria Km. 29,300 - C.P. 10 - 00016 Monterotondo Stazione, Roma, Italy

M. FINI
Istituto di Ricerca Codivilla-Putti – Istituti Ortopedici Rizzoli, Via di Barbiano, 1/10, 40136 Bologna, Italy

In this paper we describe the preparation of hydroxyfluorapatite (HFA) and fluorapatite (FA) films deposited on titanium alloys by means of the dip-coating method starting from a sol-gel prepared colloidal solution. These materials are compared with hydroxyapatite (HA) films prepared via sol gel and commercial films prepared by means of plasma spray. The film characterization from the point of view of the composition and crystallinity, performed by means of XRD, FTIR and Raman Spectroscopies, has shown a good purity degree, and compositional homogeneity for the sol-gel materials, though traces of carboxy-hydroxy apatite were found. Also, the samples exhibit a good crystallinity. SEM pictures, taken on HA coating deposited via sol-gel, revealed a homogeneous surface structure and optimum features to set up a good prosthesis-tissue interface.

1. Introduction

Ceramic coatings on metal substrates are used in several applications, with the aim of increasing the corrosion resistance of the metal or to have a higher refractory surface for high temperature applications. In the biomedical field, coatings are used to modify the implants surface and, in some cases, to create a new surface with totally different properties with respect to the substrate.

Due to the similarity with the inorganic components of the bony structure, synthetic hydroxyapatite [$Ca_{10}(PO_4)_6(OH)_2$] was one of the first materials used to coat metals. The use of hydroxyapatite as a coating is advisable, as this compound does not exhibit good mechanical properties in its bulk form. On the other hand, when the prosthesis implant is made of a metal, this can undergo corrosion processes, with consequent release of metal ions into the tissue. This is why metal implants are coated by bioactive ceramics, such as hydroxyapatite, that not only prevent corrosion, but also increase the growth rate of tissue within the pores [1].

To maintain the implant preserved in time, a good adherence is obviously required between metal substrate and coating.

Films can be deposited by means of electrophoresis, hot pressing, and sputtering methods, but actually plasma spray is the most widely used technique for these ceramic coatings. This method is nevertheless not perfectly controllable, so affecting the quality of the films obtained. To have HA with good performance once implanted it is necessary to maintain, during the deposition, the initial crystallinity, at least to 95%. Literature [2, 3] reports that plasma spray deposition in many cases induces variations in the composition and structure with respect to the starting material. These transformations bring to a considerable increase of the dissolution rate in the in vitro tests at physiologic pH. During the deposition with this technique, the starting HA is transformed into a mixture of apatite, tetracalcium phosphate and tricalcium phosphates (β-TCP and α-TCP), whose dissolution rate is very high. The same papers report that SEM analyses reveal that the surface

*Author to whom all correspondence should be addressed.

of plasma spray deposits is not uniform, but exhibits several and wide glassy areas combined with ceramic fragments having irregular shape and pores of different sizes randomly distributed; furthermore, several fractures can be observed. The formation of this surface, of such bad quality with respect to that obtained with other techniques, is due to the melting of several particles within the plasma, to their subsequent cooling and to the violent impact with the substrate.

These phenomena occur in any case, also in optimum working conditions.

The aim of this work is to study HA, fluorapatite (FA) and hydroxyfluorapatite (HFA) films prepared by the sol-gel method and to compare their behavior. Films are obtained by simple dipping of the substrate in the starting solution and intermediate films of TiO_2 and $CaTiO_3$ have been deposited to increase the adhesion. The advantages of this method, compared for example with plasma spray, are mainly due to the possibility of working at low temperature, of controlling the chemical composition of the products obtained and of getting these products with high degree of crystallinity and homogeneity.

2. Experimental

The preparation of HA, TiO_2 and $CaTiO_3$ films has been extensively described elsewhere [4].

2.1. Precursor sol for FA

To prepare the starting solution to obtain fluorapatite films (FA sol) $Ca(NO_3)_2 \cdot 4H_2O$, $(NH_4)_2HPO_4$ and NH_4F have been used as precursor salts and H_2O as the solvent, according to the following reaction [5] ($H_2NCH_2CH_2NH_2$ has been used to adjust the solution pH):

$$10\,Ca(NO_3)_2 + 6(NH_4)_2HPO_4 + 2NH_4F \rightarrow Ca_{10}(PO_4)_6F_2 + 14NH_4NO_3 + 6HNO_3$$

F^- ions are inserted in apatite network preferentially with respect to OH^- ions due to the relevant difference in ionic radius (1.68 Å for OH^- and 1.32 Å for F^-) [6].

The preparation procedure for FA sol is analogous to that for the preparation of HA sol, with four starting solution (adding NH_4F) instead of three.

2.2. Precursor sol for HFA

Two sols have been prepared for HFA containing different fluorine amounts, i.e. 25 mol % (HFA 25 sol) and 75 mol % (HFA 75 sol). Procedure and reagents are the same used for the preparation of the FA sol.

The reaction leading to the formation of hydroxyfluorapatite is the following:

$$10\,Ca(NO_3)_2 + 6(NH_4)_2HPO_4 + (2-x)H_2O + x\,NH_4F \rightarrow Ca_{10}(PO_4)_6(OH)_{(2-x)}F_x + (12+x)\,NH_4NO_3 + (8-x)HNO_3$$

where x varies between 0 and 2.

The solutions have been dried in air to be brought to suitable values of the viscosity (about 37 cps). The solutions exhibit a milky appearance. Good quality coatings are obtained stirring the solution for at least 10 minutes prior to the deposition.

2.3. Bulk characterization

To determine the working conditions to obtain the coatings, a preliminary study has been performed of the gel behavior as a function of the treatment temperature, performing several analyses on bulk samples obtained from the sols by complete drying.

Powders underwent a thermal treatment for 1 hour between 100 and 1000°C, this being the working range to obtain the coatings. The samples were characterized to determine the optimum temperatures to use for the thermal treatments of the coating. To have good quality films (especially concerning the implant lifetime), it is necessary, in fact, to have a film of high crystallinity and composition close to that of the pure compound deposited on the substrate.

The instruments used in this phase of the work include: powder X-ray diffractometer (Philips PW 1050, Cu k_α radiation), FT-IR spectrophotometer (Nicolet 5 PC), Raman spectrophotometer (LabRam), scanning electron microscope (Jeol JSM-6400), Atomic Force Microscope (ARIS 3300 Personal AFM – Burleigh Inc.), and X-rays photoelectron spectrometer (VG ESCALAB MKII).

2.4. Films preparation

All the previously described solutions have been used to prepare films by the dip-coating method, using different withdrawal rates.

Films have been deposited by "dip-coating", and after the deposition a suitable thermal treatment has been performed. A commercial titanium alloy, Ti6Al4V, known to have very good mechanical properties and good resistance to corrosion, has been used as the metal substrate.

To allow the characterization of the samples by means of the previously described analytical techniques, the substrate has been cut into pieces having dimensions $10 \times 10 \times 1$ mm^3. These have then been lapped in order to reduce as much as possible the border effect that might affect the quality of the film.

Subsequently, the substrates have been rinsed first with water, then with acetone, and dried in air, under laminar flow to avoid the deposition of dust particles. A preliminary thermal treatment has then been performed at 400°C for 15 minutes to remove any trace of organics from the surface.

A single dip-coating process from the TiO_2 sol has given rise to the film of titanium oxide. The solvent has been evaporated at room temperature for 10 minutes under laminar flow, and then the final treatment has been performed in an electric furnace up to 750°C.

A single layer has been deposited also for calcium titanate, starting from $CaTiO_3$ sol. Solvent evaporation has been obtained as above and the final treatment has been performed again at 750°C.

Two layers have been deposited to prepare apatite films. After each deposition the samples have been let for 30 minutes under laminar flow to let the solvent evaporate, and then heat-treated in a furnace.

The first layer has been deposited using a withdrawal rate of 19.5 cm/min, the second at 12.4 cm/min. After the first deposition, the film has been completely dried with a preliminary treatment, i.e. a gradual heating up to 200°C. After the second deposition, the samples have been heated up to 600°C and let to cool in the furnace to avoid crack formation due to thermal shock.

3. Results

Before characterizing the different forms of apatite prepared, the materials to be used as intermediate have been tested. The analysis performed on TiO_2 bulk reveal a good degree of crystallinity and confirm the complete formation of the network [7, 8]. For what concerns $CaTiO_3$ [9, 10], starting from 500°C only the peaks of the perovskite form $CaTiO_3$ are present, while at 750°C another phase of calcium titanate, having formula $Ca_2Ti_5O_{12}$, appears.

Regarding the characterization of the forms of apatite, the diffractograms obtained for HA, FA and HFA are absolutely correspondent: this can be ascribed to the fact that the substitution of OH^- ions by F^- ions does not induce a relevant variation in the distance between the planes in the network. Fig. 1 shows that untreated

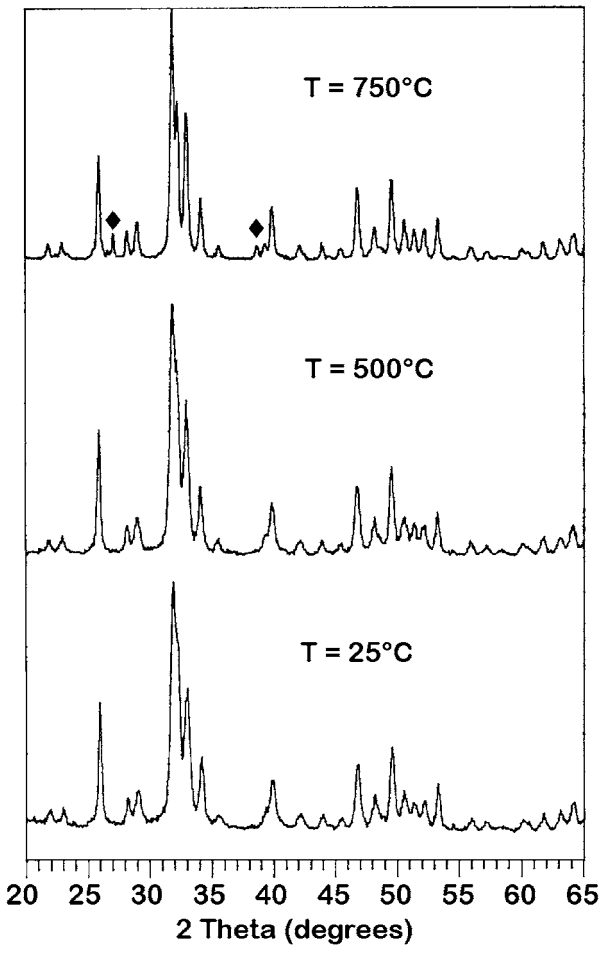

Figure 1 Thermal evolution of hydroxyapatite (♦= β-$Ca_3(PO_4)_2$).

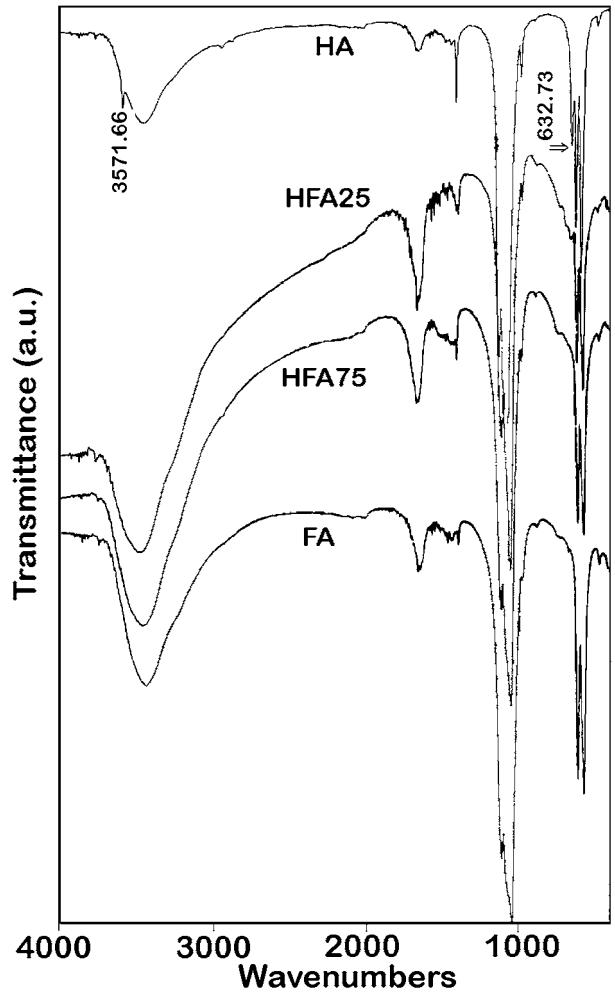

Figure 2 IR spectra of HA, HFA's and FA.

apatite already exhibits a certain degree of crystallinity. Increasing the temperature, the crystallinity increases starting from 600°C.

At 750°C peaks belonging to the phase β-$Ca_3(PO_4)_2$ appear: it should be better to prevent the formation of this phase due to its greater solubility with respect to pure apatite. This is why the thermal treatments on the apatite coatings will not be performed above 600°C.

Fig. 2 reports IR spectra. For hydroxyapatite, the main signals are attributed as follows: 3571.66 cm^{-1} O-H, 1094.74, 1037.83 and 962.60 cm^{-1} P-O, 632.73 cm^{-1} Ca_3-OH, 603.80 and 567.14 cm^{-1} PO_4 tetrahedra. A sharp peak is recorded around 1410 cm^{-1} and a very weak one at about 870 cm^{-1}. According to A. Jillavenkatesa *et al.* [11], these signals are to be ascribed to carbonate-hydroxyapatite. This indeed could be formed inside the material due to the use, in the preparation, of $H_2NCH_2CH_2NH_2$ and the subsequent treatment in air atmosphere.

Considering the spectra of HFA 25, HFA 75 and FA, there are obviously a few variations with respect to HA in the bands involving vibration modes of OH. As fluorine content increases, the peak moves towards lower frequencies, being hidden by the larger band centered at 3432.76 cm^{-1}, due to OH belonging to water. This is why a study of the peak at 632.73 cm^{-1} is preferred. The signal at 632.73 cm^{-1} in hydroxyapatite is due to OH's immersed in an infinite chain of OH, while this chain is interrupted by F's in the other compounds:

this band decreases in intensity and is shifted to higher frequencies, meaning that there is a strong coupling among the dipoles of OH's along the chain. The phenomenon is rather clear passing from HA to HFA 25 and HFA 75 (the band shifts from 632.73 to 633.51 and 634.23 cm^{-1}), while HFA 75 and FA seem substantially the same; probably, fluorine atoms are so numerous in the chain, already in HFA 75, that prevent OH's from a reciprocal interaction. The previously described signal around 1410 and 870 cm^{-1} are still present, even if weaker (especially for the former) than in the HA case.

As Raman spectra are not largely influenced by water, it is easier to follow their transformation passing from HA to FA through HFA, also at high frequencies. The most interesting zone of the spectra is that around 3500–3650 cm^{-1} (Fig. 3): it is possible to notice the transformation of the band at 3575 cm^{-1} in the spectrum of HA, due to the stretching of OH's inserted in an infinite chain of OH's. Passing to HFA25, the intensity of this signal decreases and a broad band appears at lower frequencies (about 3540 cm^{-1}), due to the stretching of OH's linked to F's through hydrogen bonds. For HFA75 the signal at 3575 cm^{-1} has disappeared, so all the OH's present are linked to F's through hydrogen bonds. Both these bands disappear passing to FA, i.e. there are no OH's present in the chain any longer.

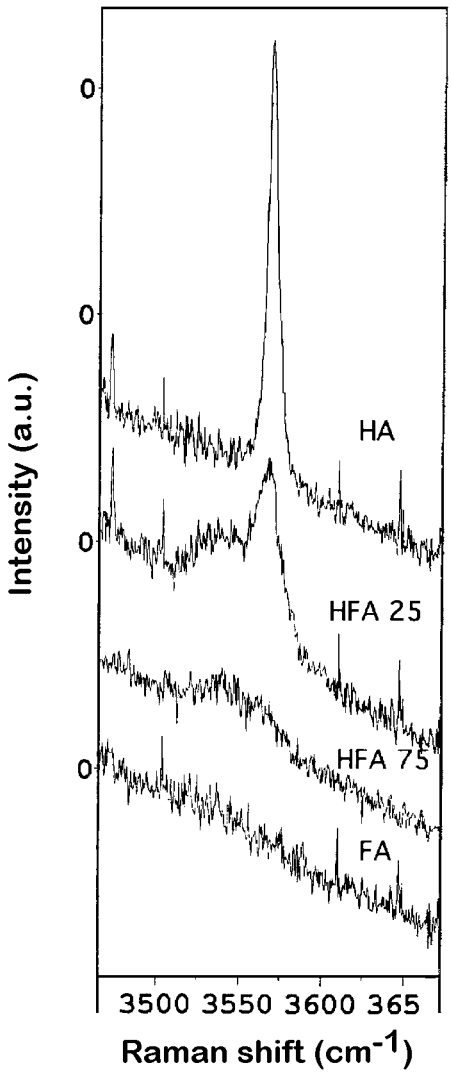

Figure 3 Raman spectra of HA, HFA's and FA.

TABLE I Relative atomic concentration for the various elements

Sample	C 1s	O 1s	Ca 2p	P 2p	F 1s
HA	0.55	1.76	1.00	0.38	—
HFA 25	0.81	2.05	1.00	0.40	0.03
FA	0.85	1.56	1.00	0.34	0.14

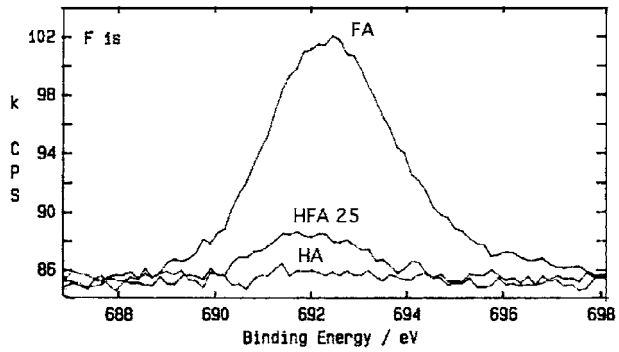

Figure 4 XPS spectrum of fluorine.

XPS analyses have been performed on HA, HFA 25 and FA films deposited on silica substrates. Fig. 4 shows XPS spectrum for fluorine, while Table I reports the atomic amounts of the various elements normalized with respect to calcium.

As expected, the amount of phosphorous is approximately the same for the three samples.

The presence of carbon and the trend of the oxygen content, different from that expected (HA > HFA 25 > FA), also indicates the presence of apatite carbonate, as already seen from IR spectra.

Last, the amount of fluorine is, as expected, equal to zero in HA and increases passing to HFA 25 and FA. Furthermore, assuming to have for FA a complete substitution of OH by F, i.e. $x = 0$ (100 % F) in the formula $3Ca_3(PO_4)_2\ CaOH_xF_{2-x}$, in HFA 25 the substitution degree is calculated as $x = 1.56$ (22 % F), close to the expected value $x = 1.50$ (25 % F).

3.1. Characterization of hydroxyapatite deposited by plasma spray

The samples for XRD, IR and Raman analyses have been obtained by scratching the surface of a commercial hip prosthesis made of steel coated by plasma sprayed hydroxyapatite.

XRD analysis (Fig. 5) reveals, with respect to that performed on sol-gel prepared hydroxyapatite, a lower degree of crystallinity and the presence of peaks attributable to the presence of β - $Ca_3(PO_4)_2$ and other unidentified.

Fig. 6 reports the IR spectrum. One can notice the absence, at about 3570 cm^{-1}, of the absorption signal due to the stretching of OH, maybe too weak and so hidden by the absorption of water. The bands expected at 560–640 cm^{-1} and 962–1095 cm^{-1} are not well defined as in the case of sol-gel prepared hydroxyapatite. This phenomenon can be ascribed to the low crystallinity of the sample.

Last, Fig. 7 shows two Raman spectra recorded in two different points of the sample. The first (Fig. 7a)

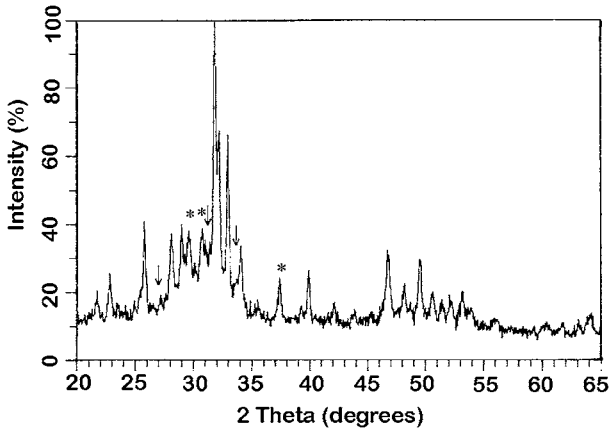

Figure 5 X-ray diffractogram of HA deposited by plasma spray ($* = \beta$-$Ca_3(PO_4)_2$, $\downarrow$ = unknown).

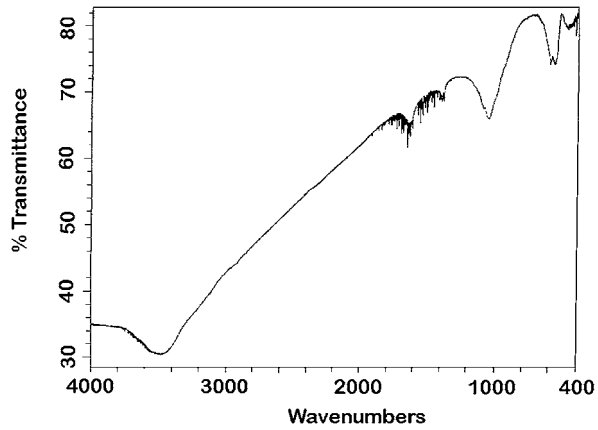

Figure 6 IR spectrum of HA deposited by plasma spray.

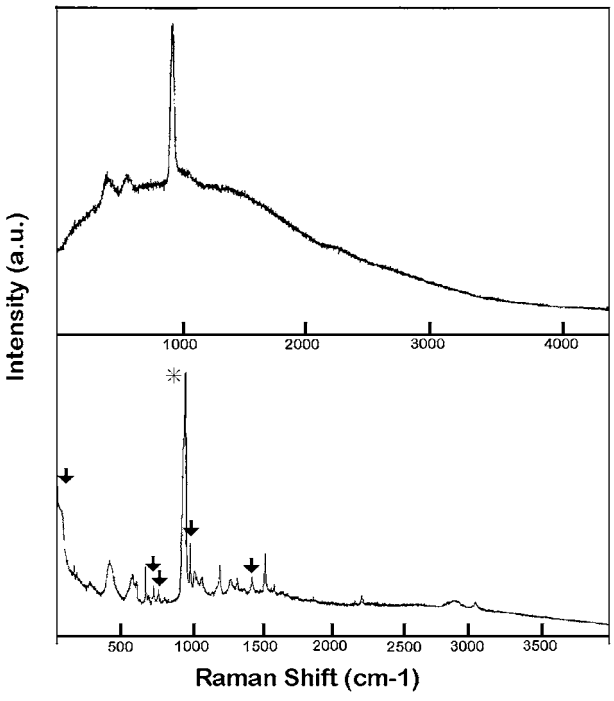

Figure 7 Raman spectra of HA deposited by plasma spray. Top: grain border; bottom: inside the grain. ($* = \beta$-$Ca_3(PO_4)_2$, $\downarrow$ = unknown).

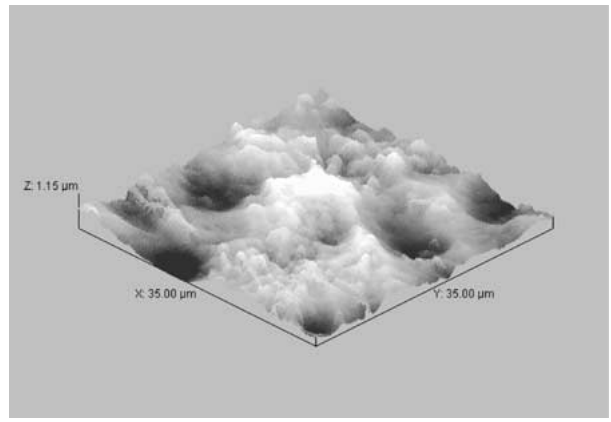

Figure 8 AFM image of the metal substrate treated at 400°C.

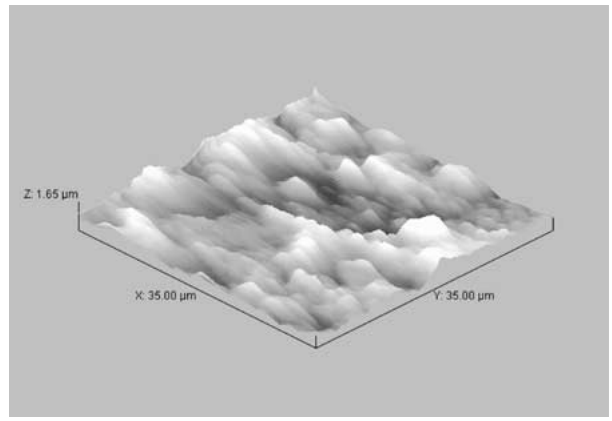

Figure 9 AFM image of the metal substrate treated at 750°C.

has been recorded on the surface of a grain come off the prosthesis and one can see that the background noise is very high, so that the spectrum is hard to read. Better results are obtained by breaking the grain and analyzing it inside (Fig. 7b). This indicates that the sample exhibit a great inhomogeneity: also, in this case, as seen for IR spectrum, there is no signal due to OH (at 3575 cm^{-1}), and, besides the expected bands, there is an absorption attributable to calcium phosphate at 952 cm^{-1} and other bands which have not been assigned.

3.2. Characterization of the films

SEM and AFM analyses have been performed in various zones of the films and the average results have been considered. The study of the morphology takes into account three fundamental parameters necessary to guarantee a good performance of the implant: surface homogeneity, adherence to the metal substrate (absence of cracks), surface area high enough to allow the growth of the tissues inside the pores of the apatite film.

3.3. Preliminary characterization of the substrate

From SEM analyses performed on the metal substrate, it is possible to observe that the alloy Ti6Al4V treated at 400°C for 10 minutes exhibits a very irregular surface: one can see flat zones alternated with round shaped cavities with diameter varying from 1 μm to 10 μm.

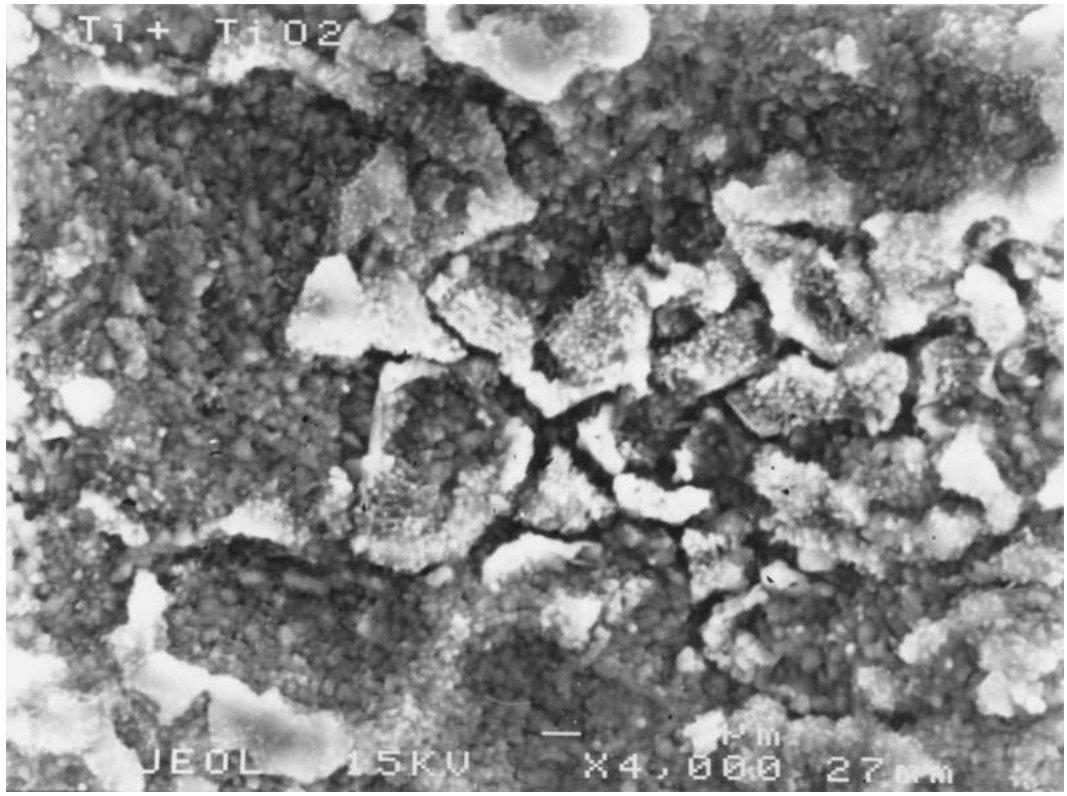

Figure 10 SEM picture of the TiO_2 film (×4000).

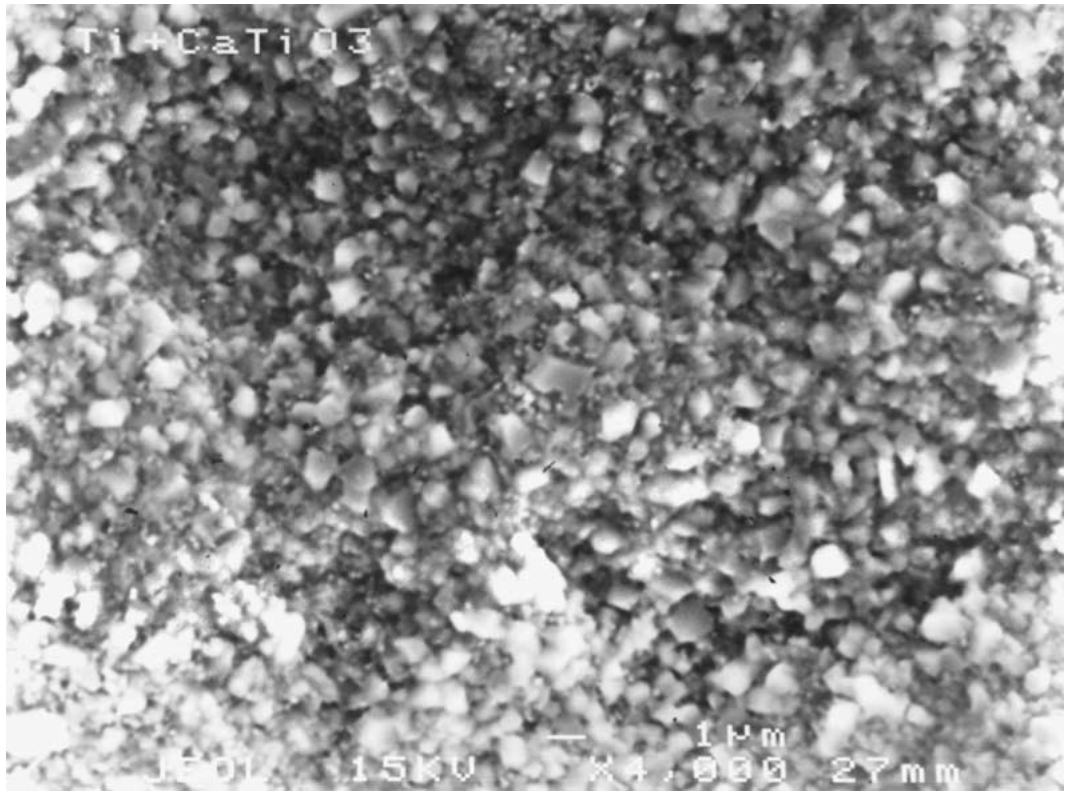

Figure 11 SEM picture of the $CaTiO_3$ film (×4000).

The AFM image (Fig. 8) reveals that the depth of the cavities is about 450 nm.

The surface of the uncoated substrate has been analyzed also after a thermal treatment at 750°C. In fact, the films of TiO_2 and $CaTiO_3$ deposited before the thermal treatment are thin enough to allow the diffusion of oxygen towards the underlying metal surface, so causing its oxidation. SEM pictures show that the surface does not exhibit round cavities regularly distributed, while it is possible to notice the occurred formation of particles having different dimensions (from few nm to 5–6 μm), probably made of titanium oxidized products.

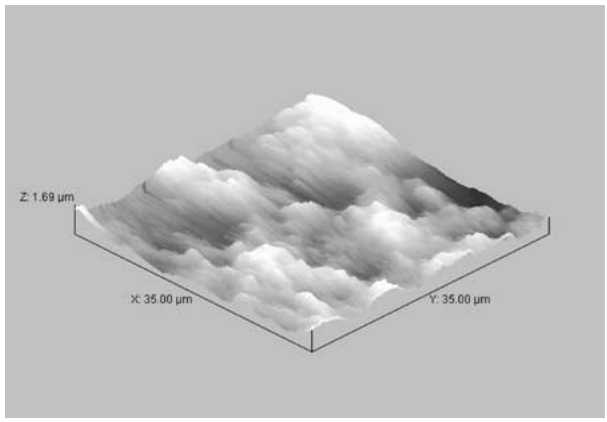

Figure 12 AFM image of the $CaTiO_3$ film.

This morphological trend is evident from three-dimensional AFM image (Fig. 9). The surface analysis shows that the surface is somehow flattened: the cavities, in fact, have been filled by TiO_x. The formation of surface oxides upon heating is confirmed by XRD analyses performed on the metal substrate treated at 400°C, in which only elemental titanium is evident, and at 750°C, where other peaks appear, due to anatase and rutile. The surface oxidation of the metal substrate upon heating in air is confirmed also by an XPS study [3].

3.4. Characterization of TiO_2 film

The SEM image (Fig. 10) shows a certain inhomogeneity of the film: in fact, particle sizes vary in the range between a few nanometers and 10 μm, furthermore one can notice the presence of rather deep cracks between the particles, that might affect the adherence of the film.

3.5. Characterization of $CaTiO_3$ film

With respect to previous observations, SEM analysis reveals a good homogenization of the surface, similar to that of a living tissue. The most magnified image (×4000, Fig. 11) allows to value the homogeneity of $CaTiO_3$ film; all the particles, in fact, have comparable dimensions, of about 1 μm. In some points a few hexagonal perovskite crystals appear. The AFM 3D image (Fig. 12), differently from the bidimensional SEM picture, shows the presence of a certain porosity.

From these analyses one can deduce that the best intermediate film to have a good adherence, homogeneity and porosity of the apatite film is certainly $CaTiO_3$.

The next step, so, has dealt with SEM and AFM analyses of HA films deposited on a $CaTiO_3$ layer.

3.6. Characterization of the hydroxyapatite film

SEM analysis (Fig. 13) shows that the surface exhibits morphology similar to that of the bony tissue [12]. Magnification is not high enough to distinguish the single hydroxyapatite particles; in fact, only from AFM image (Fig. 14), at high magnification, one can see that these particles have dimensions of 200–350 nm, as expected from a suspension of colloidal particles obtained via sol-gel. From SEM pictures one can see various cavities, homogeneously distributed, with diameter variable between 5 and 10 μm. In this way the coated prosthesis exhibits a surface having good homogeneity and large area, so allowing the formation of a wide zone in contact with the living tissue. Furthermore, thanks to the cavities on the hydroxyapatite film, the tissue, besides growing inside them, can be fed by blood capillaries.

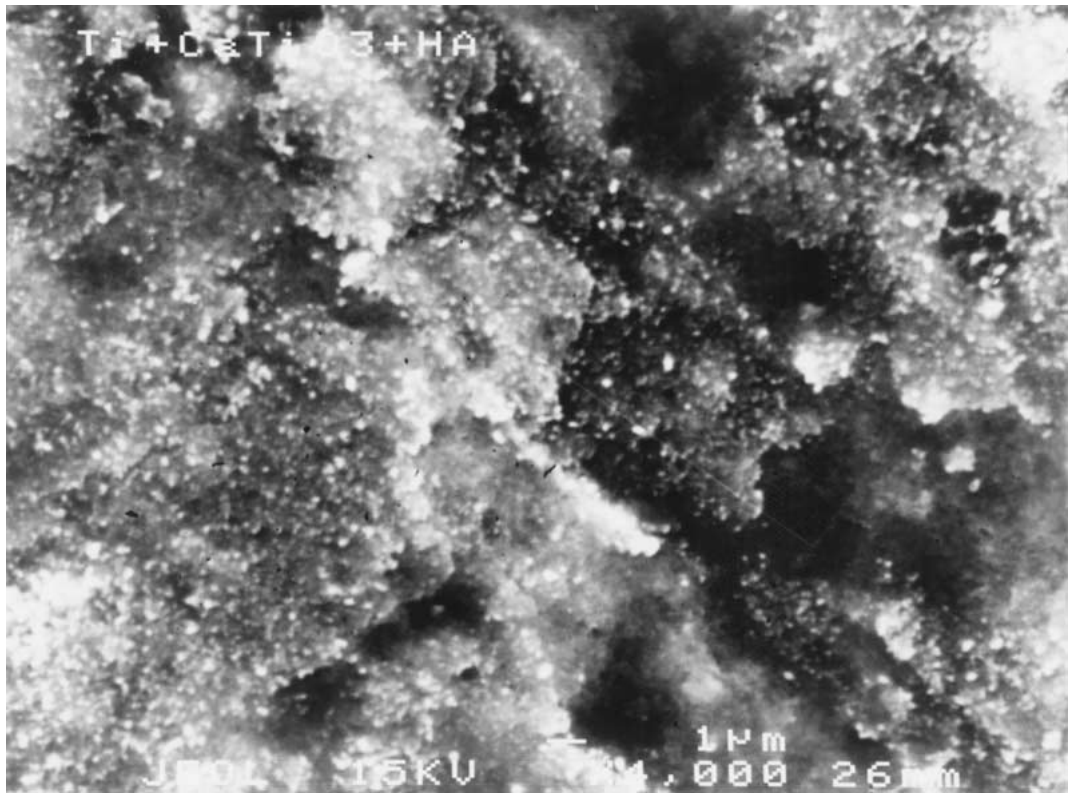

Figure 13 SEM picture of the sol-gel deposited HA film (×4000).

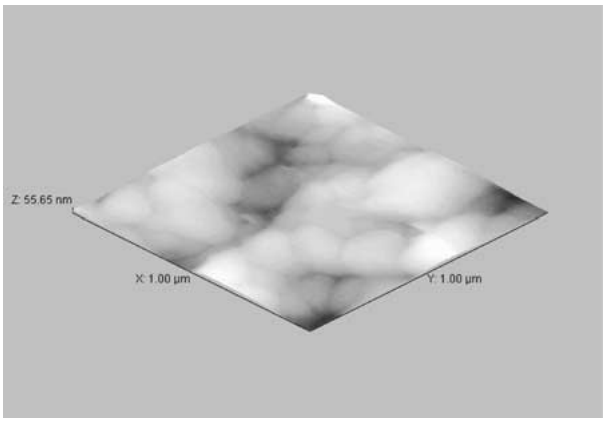

Figure 14 AFM image of the sol-gel deposited HA film.

Comparing these images with others reported in literature (see for example [13]) regarding a hydroxyapatite surface deposited by the plasma spray commercial technique, it is easy to see the absolute surface inhomogeneity of the HA deposited with this latter method. Furthermore, in these latter samples one can note that crystalline areas are alternated with glassy ones, due, as previously said, to the sudden cooling during the passage from plasma (10.000°C) to the metal substrate (200–300°C). Also, there are cracks due to the violent impact of HA particles with the material to coat.

4. Conclusions

In this work we tested the application of the sol-gel technique to the realization of ceramic coatings on metals to obtain composite biomaterials to be used in the fabrication of orthopedic prostheses.

The studies have been concentrated on the preparation of hydroxyapatite films, fluorapatite and hydroxyfluorapatite on a substrate of Ti6Al4V alloy deposited by dipping.

From the study of the bulk, by means of the techniques IR, Raman, XRD and XPS, it was possible to see the presence of apatites having different purity and crystallinity degree, qualities that give the films a very good resistance to degradation and a good biocompatibily as a implant.

From the morphological surface analyses, performed on the films by means of SEM and AFM, it was possible to identify the substrate having the best features concerning the surface quality. As a first result we concluded that the best intermediate layer between metal and apatite is the one based on $CaTiO_3$, which exhibits a better homogeneity and adherence to the titanium alloy, with respect to that of TiO_2. As for the apatite films, both that based on HA and on FA exhibit a very good homogeneity, but only the HA film shows a porosity degree high enough to allow the growth of tissues inside the pores themselves, so setting up a very wide contact surface between tissue and prosthesis.

The sol-gel process has not found an industrial application yet in the field of biomaterials. At present only the plasma spray method is used for the deposition, but we have seen that the results are worst, from the points of view of purity, crystallinity and surface homogeneity, with respect to those obtained from sol-gel. On the other hand, the commercial technique allows to obtain films of relevant thickness (40–60 μm) always maintaining a very good adherence and furthermore, during the treatment the metal substrate does not reach more than 300°C.

To demonstrate the potential competitiveness of the sol-gel technique for biomedical applications it is necessary to achieve in the future the following scopes:

1. Realization of film with thickness comparable to those produced by means of plasma spray, having a good adherence to the metal substrate;
2. Study of the variations with temperature of the mechanical properties of the alloys used for prosthetic implants and, if necessary, new evaluation of the thermal ramps used in this work, trying to obtain at the same time a implant with good mechanical properties and a coating with hydroxyapatite crystalline enough to guarantee a long duration in the implant.

Acknowledgements

The authors would like to thank the Company Comepre (Milan, Italy), for supplying the alloy Ti6Al4V used as the substrate and Centro di Strutturistica Diffrattometrica of National Research Council (Parma) for making X-ray Powder diffractometer available for the analyses.

This work was performed in the frame of the Targeted Project "Materiali Speciali per Tecnologie Avanzate II" of Italian CNR.

References

1. L. L. HENCH and J. WILSON, in "An Introduction to BIOCERAMICS," edited by L. L. Hench, J. Wilson (World Scientific, Singapore - New Jersey - London - Hong Kong, 1993), p. 1.
2. S. R. RADIN and P. DUCHEYNE, *J. Mat. Science: Materials in Medicine* **3** (1992) 33.
3. F. CIRILLI, S. KACIULIS, G. MATTOGNO, G. RIGHINI, F. FERRARI, A. MONTENERO and G. GNAPPI, "ECASIA 97," edited by J. Olefjord, L. Nyborg and D. Briggs (John Wiley & Sons, Chichester (UK), 1997) p. 151.
4. A. MONTENERO, F. FERRARI, M. CESARI, G. GNAPPI, E. SALVIOLI, L. MATTOGNO, S. KACIULIS and M. FINI, *J. Mater. Sci.* **35** (2000) 2791.
5. T. S. B. NARASARAJU, *Indian J. Chem.* **10** (1972) 309.
6. T. S. B. NARASARAJU, R. P. SINGH and V. L. N. RAO, *ibid.* **8** (1970) 296.
7. D. BERSANI, G. ANTONIOLI, P. P. LOTTICI and T. LOPEZ, *J. Non-Cryst. Solids* **234** (1998) 175.
8. R. GOMEZ, *Materials Chemistry and Physics* **32** (1992) 141.
9. U. BALACHANDRAN and N. G. EROR, *Solid State Communications* **44** (1982) 815.
10. C. H. PERRY, B. N. KHANNA and G. RUPPRECHT, *Physical Review* **135** (1964) 408.
11. A. JILLAVENKATESA, D. T. HOELZER and R. A. CONDRATE, SR., *J. Mater. Sci.* **34** (1999) 4821.
12. W. HÖLAND and W. VOGEL WILSON, in "An Introduction to BIOCERAMICS," edited by L. L. Hench and J. Wilson (World Scientific, Singapore - New Jersey - London - Hong Kong, 1993), p. 132.
13. W. R. LACEFIELD WILSON, in "An Introduction to BIOCERAMICS," edited by L. L. Hench and J. Wilson (World Scientific, Singapore - New Jersey - London - Hong Kong, 1993), p. 228.

Received 28 March
and accepted 8 November 2000